

## EFFECT OF SOLUTION TREATMENT ON MECHANICAL PROPERTIES OF CAST AZ91-(Ca) ALLOYS

Effects of solution treatment on room temperature mechanical properties were studied in cast AZ91 (Mg-9%Al-1%Zn-0.2%Mn) and AZ91-0.5%Ca alloys. In as-cast state, the Ca addition contributed to the suppression of discontinuous  $\beta$  phase precipitation and the formation of  $Al_2Ca$  phase. After solution treatment, the AZ91 alloy had only a small amount of  $Al_8Mn_5$  particles, while  $\beta$  and  $Al_2Ca$  phases were still present in the Ca-containing alloy. In as-cast state, the AZ91-0.5%Ca alloy showed better yield strength and hardness than the AZ91 alloy. The solution treatment increased the elongation in both alloys, which eventually led to the increase in ultimate tensile strength. The solution treatment resulted in a marked decrease in yield strength and hardness in the AZ91 alloy, whereas the decrements in those values were relatively negligible in the Ca-containing alloy due to the residual phases and solution hardening effect of Ca.

*Keywords:* AZ91 alloy, calcium, mechanical properties, microstructure, solution heat treatment

### 1. Introduction

Mg alloys are the lightest structural materials that have great potential for use in the automotive industry, where lightweight materials are preferred because of their ease of transport and the consequent reduction in costs [1,2]. However, widespread utilization of Mg alloys is limited by their inferior strength and ductility in comparison with those of Al and Ti alloys. In previous works, it was reported that the addition of Ca can increase the strength at room and elevated temperatures in the Mg-Al based alloys because its addition results in the formation of Ca-containing intermetallic compounds with higher thermal stability such as  $Al_2Ca$ ,  $Mg_2Ca$  and  $(Mg,Al)_2Ca$  [3-5]. Although numerous researches have been performed on the Mg-Al-Ca alloys [6-11], most of them have only dealt with the alloys in the as-cast and aged states. Thus, there is little information available on the mechanical properties of the solution-treated alloy. Since most of the Mg-Al based alloys are heat-treatable and their properties are greatly affected by microstructural evolution depending on heat treatment conditions [7,8,12], it is necessary to examine the dependence of mechanical properties on solution treatment in the Mg-Al-Ca alloys. This work aims to investigate the effects of solution treatment on the microstructure and room temperature mechanical properties of AZ91 alloys considering Ca addition.

### 2. Experimental

Two alloys, AZ91 alloys having 0 and 0.5% of Ca (wt%), were prepared by melting the commercial AZ91 billets and 99.0%Ca under a ( $SF_6 + CO_2$ ) protective gas environment and casting the alloys in a metallic mold. From the ingots, various specimens for microstructural characterization and mechanical tests were prepared by machining. The chemical compositions of experimental alloys were determined by inductively coupled plasma (ICP) analysis, and the results are listed in Table 1. Some samples were solution-treated at 413°C for 16 h, followed by quenching in water at room temperature. Uniaxial tensile tests were carried out at room temperature on universal testing machine (UTM, Shimadzu AG-250 kN) at a constant crosshead speed of 1 mm/min. ASTM subsize specimens with a gauge length of 25 mm were used in this study. The hardness was measured by means of Vickers micro-hardness tester (Shimadzu HMV-2) with a load of 200 gf. The microstructure was characterized by X-ray diffractometry (XRD, Bruker-AXS D8 Discover, Cu-K $\alpha$  radiation) and field-emission scanning

TABLE 1

Chemical compositions of experimental alloys (wt%)

Composition	Al	Zn	Mn	Ca	Mg
AZ91	8.7	0.65	0.25	—	bal.
AZ91-0.5%Ca	8.5	0.57	0.23	0.46	bal.

\* KOREA INSTITUTE OF INDUSTRIAL TECHNOLOGY, ADVANCED PROCESS AND MATERIALS R&D GROUP, INCHEON 21999, REPUBLIC OF KOREA

# Corresponding author: jhjun@kitech.re.kr

electron microscopy (FE-SEM, FEI QUANTA-200F) combined with energy dispersive X-ray spectroscopy (EDS, AMETEK PV72-60030F).

### 3. Results and discussion

Fig. 1 shows the SEM images of the AZ91 and AZ91-0.5%Ca alloys in the as-cast and solution-treated states. In the as-cast state, the AZ91 alloy exhibits a dendritic microstructure containing partially divorced eutectic  $\beta$  ( $\text{Mg}_{17}\text{Al}_{12}$ ) particles along the dendrite cell boundaries and discontinuous  $\beta$  precipitates with a fine lamellar morphology adjacent to the eutectic  $\beta$  particles, as seen in Fig. 1-(a). The addition of 0.5%Ca slightly refines the eutectic  $\beta$  phase and contributes to the suppression of discontinuous  $\beta$  precipitation (Fig. 1-(b)). This microstructural change is in good agreement with previously reported results and is typical of Mg-Al-Ca alloys [6,9]. The microstructure

refinement caused by Ca addition is related to the strong segregation behavior of Ca solutes, which induces constitutional undercooling in a diffusion layer ahead of the advancing solid/liquid interface and restrains the growth of the cells [13]. The suppression of discontinuous  $\beta$  precipitation and the refinement of eutectic  $\beta$  phase in the Ca-containing alloy are resulted from a decrease in the amount of Al engaged in the eutectic reaction. This reduction is caused by the formation of an  $\text{Al}_2\text{Ca}$  phase prior to the eutectic reaction that results in a decrease in Al content in the diffusion layer [14]. After solution treatment for 16 h at  $413^\circ\text{C}$ , the  $\beta$  particles are completely dissolved into the  $\alpha$ -(Mg) matrix, and only trace amount of  $\text{Al}_8\text{Mn}_5$  particles, with their high melting point of  $1048^\circ\text{C}$ , are found in the AZ91 alloy as seen in Fig. 1-(c) [15]. Notably, after solution treatment, a relatively large amount of compound particles can still be observed in the Ca-containing alloy (Fig. 1-(d)). The volume fractions of the intermetallic compound particles, measured using image analysis, were  $\sim 15\%$  (as-cast) and  $\sim 0.5\%$  (solution-treated) in

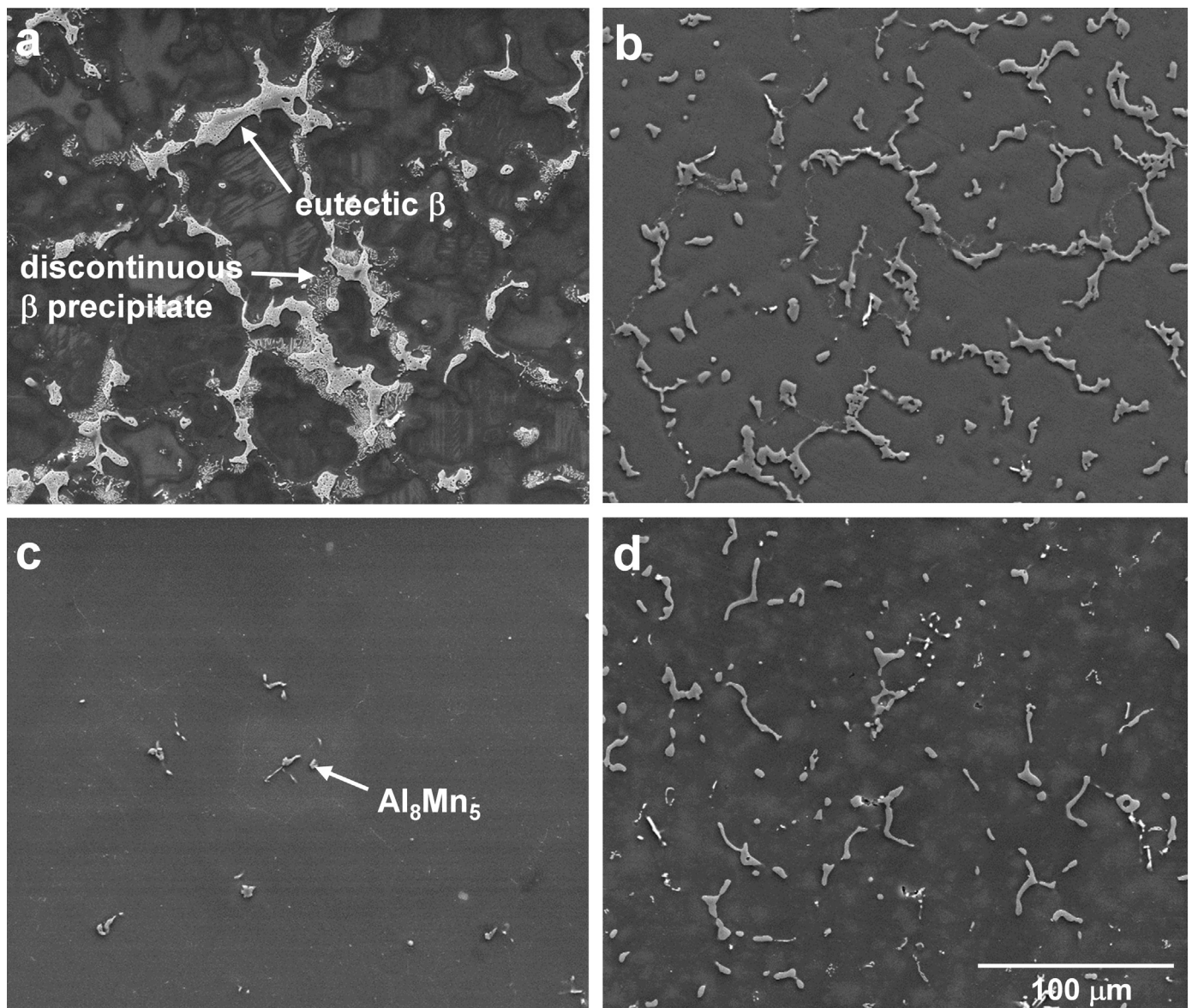


Fig. 1. SEM microstructures of (a) as-cast AZ91, (b) as-cast AZ91-0.5%Ca, (c) solution-treated AZ91 and (d) solution-treated AZ91-0.5%Ca alloys

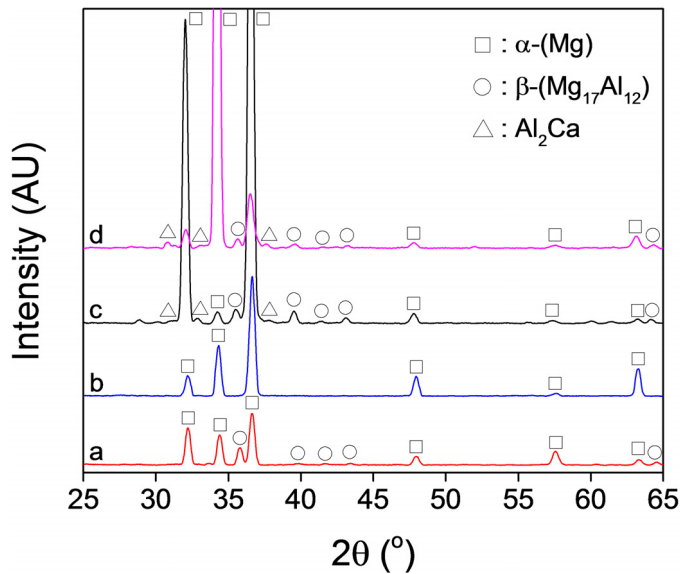


Fig. 2. XRD patterns of AZ91 and AZ91-0.5%Ca alloys: (a) as-cast AZ91, (b) solution-treated AZ91, (c) as-cast AZ91-0.5%Ca and (d) solution-treated AZ91-0.5%Ca alloys

the AZ91 alloy and  $\sim 14\%$  (as-cast) and  $\sim 7\%$  (solution-treated) in the AZ91-0.5%Ca alloy. In order to clarify the phase constituents in the as-cast and solution-treated AZ91 and AZ91-0.5%Ca alloys, the microstructures were further characterized by XRD and EDS, and the results are given in Figs. 2 and 3. Fig. 2 shows XRD patterns of the AZ91 and AZ91-0.5%Ca alloys in the as-cast and solution-treated states. It is observed that the AZ91 alloy is mainly composed of  $\alpha$ -(Mg) and  $\beta$  phases (Fig. 2-(a)), and that the addition of 0.5%Ca into the AZ91 alloy results in the formation of additional  $\text{Al}_2\text{Ca}$  phase in the microstructure (Fig. 2-(c)). After the solution treatment, only  $\alpha$ -(Mg) phase peaks are seen in the AZ91 alloy (Fig. 2-(b)), but several peaks corresponding to  $\beta$  and  $\text{Al}_2\text{Ca}$  phases are still observed in the AZ91-0.5%Ca alloy (Fig. 2-(d)). The XRD patterns in Fig. 2 indicates that regardless of the solution treatment, the AZ91-0.5%Ca alloy contains  $\text{Al}_2\text{Ca}$  phase, even though its presence is not noticeable in Fig. 1. Enlarged SEM images and EDS elemental maps of the intermetallic compound particles in the as-cast and solution-treated AZ91-0.5%Ca alloy are shown in Fig. 3. It is found from the EDS maps that the compound particles observed in the as-cast and solution-treated AZ91-0.5%Ca alloy are Ca-containing  $\beta$  phase and  $\text{Al}_2\text{Ca}$  phase (some Mg-poor, Al-rich and Ca-rich areas). The EDS compositional analysis results of areas “A” to “D” in Fig. 3 are listed in Table 2, which confirms the presence of  $\text{Al}_2\text{Ca}$  (“A” and “C”) and Ca-containing  $\beta$  (“B” and “D”) phases in the as-cast and solution-treated AZ91-0.5%Ca alloy. The existence of  $\text{Al}_2\text{Ca}$  particles following solution treatment is reasonable because the melting point of  $\text{Al}_2\text{Ca}$  is high,  $1079^\circ\text{C}$  [16], thus impeding particle dissolution. The  $\beta$  phase retained in the AZ91-0.5%Ca alloy after the solution treatment implies that thermal stability of the  $\beta$  phase is significantly improved by the inclusion of Ca. The increase in the melting point of the  $\beta$  phase containing Ca was demonstrated using differential thermal analysis (DTA)

by Min et al. [17]. The authors explained that the addition of Ca results in a more uniform distribution of valence electrons within the dominant bonds and unit cell, leading to an increase in the melting point of the  $\beta$  phase.

TABLE 2

EDS analysis results of areas A, B, C and D in Fig. 3

Area	Amount of alloying element (at%)				
	Mg	Al	Zn	Ca	Mn
A	15.6	57.8	1.3	25.1	0.2
B	62.9	32.7	2.3	1.9	0.2
C	12.3	58.9	1.2	27.5	0.1
D	62.2	33.5	2.2	2.0	0.1

Fig. 4 shows the Vickers micro-hardness values of the AZ91 and AZ91-0.5%Ca alloys in the as-cast and solution-treated states. In the as-cast state, the AZ91-0.5%Ca alloy has a higher hardness than the AZ91 alloy. After the solution treatment, a remarkable decrease in hardness is observed in the Ca-free alloy, while the decrement is negligible in the case of the Ca-containing alloy. The engineering stress-strain curves at room temperature of the AZ91 and AZ91-0.5%Ca alloys in as-cast and solution-treated states are shown in Fig. 5, and the YS, UTS, and elongation values obtained from Fig. 5 are listed in Table 3. In the as-cast state, the Ca-containing alloy has higher YS and lower elongation than the Ca-free alloy, attributable to the combined effects of microstructure refinement, formation of Ca-based intermetallic compounds, and solid solution hardening of Ca [6,9]. The solution treatment increases the elongation in the AZ91 and AZ91-0.5%Ca alloys due to the complete and partial dissolution of the  $\beta$  phase, respectively, which eventually leads to the increase in UTS in both alloys. After the solution treatment, decrements in YS and hardness of the Ca-containing alloy are much smaller than those of the Ca-free alloy. A previous report by Gharghouri et al. [18] demonstrates that strengthening by  $\beta$  phase has more influence on the YS value than other strengthening mechanisms in the AZ91 alloy. Therefore, the retained YS and hardness values in the Ca-containing alloy are likely the results of dispersion hardening by the residual compound particles with improved thermal stability and solution hardening by Ca solutes in part. When compared to the as-cast AZ91 alloy, the solution-treated AZ91-0.5%Ca alloy exhibits increased YS, UTS, hardness, and elongation values by 3.9%, 33.7%, 0.8%, and 52.0%, respectively. The solution treatment may improve the elongation and UTS in the as-cast AZ91 alloy, but it definitely causes deterioration in YS and hardness to some extent, as shown in Fig. 5 and Table 3. In addition, it is well known that aging treatment results in the enhancement of YS; however, in such a case, considerable loss in ductility is inevitable [12]. The better ductility of the solution-treated alloy compared to the as-cast one is directly ascribed to the lower content of intermetallic phases such as  $\beta$  and  $\text{Al}_2\text{Ca}$  with a brittle nature, since the intermetallic particles are the micro-crack initiators during deformation [19]. If the interfacial cohesion

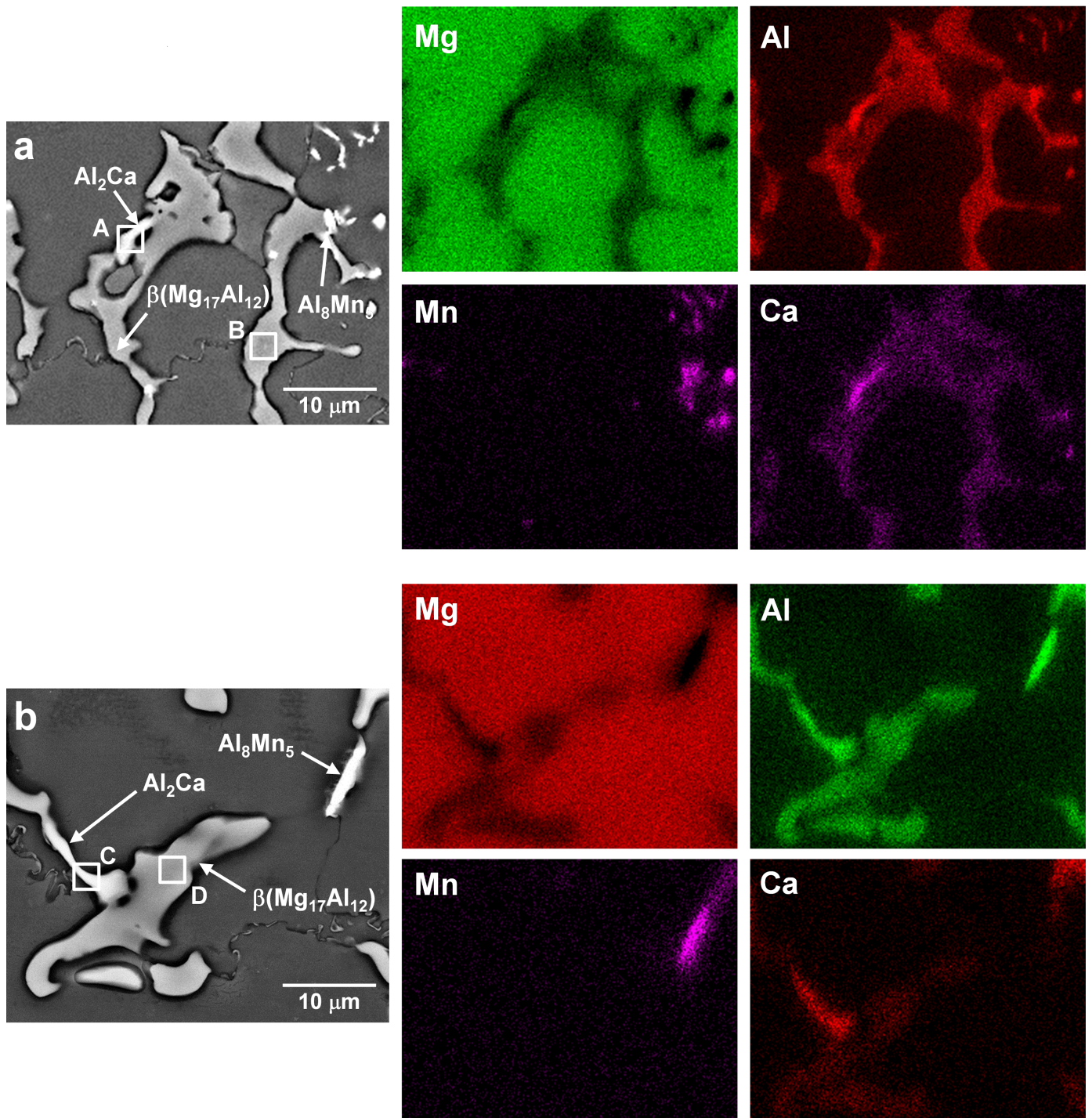


Fig. 3. SEM images showing precipitate particles (left) and EDS maps of the elements Mg, Al, Mn and Ca (right) in (a) as-cast and (b) solution-treated AZ91-0.5%Ca alloy

TABLE 3

Room temperature tensile properties of AZ91 and AZ91-0.5%Ca alloys in as-cast and solution-treated states. AC and ST denote as-cast and solution-treated states, respectively

Alloy	Tensile properties		
	YS (MPa)	UTS (MPa)	Elongation (%)
AZ91 (AC)	76	181	5.0
AZ91-0.5%Ca (AC)	84	182	4.5
AZ91 (ST)	63	228	8.1
AZ91-0.5%Ca (ST)	79	242	7.6

between the intermetallic particles and matrix are strong, the particles will fracture to nucleate micro-cracks, and when the interfacial cohesion is weak, decohesion will happen to nucleate micro-cracks. This study demonstrates that the combination of a small Ca addition and solution treatment can play a beneficial role in enhancing UTS and elongation of the AZ91 alloy without any reduction in YS and hardness.

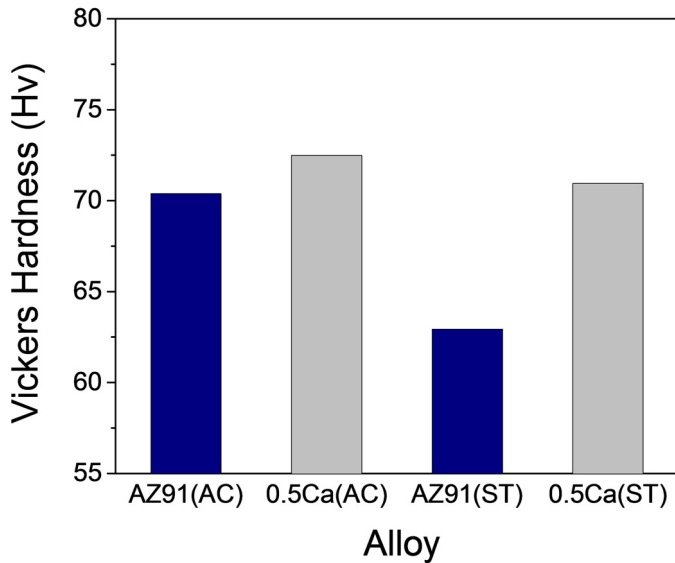


Fig. 4. Vickers micro-hardness of AZ91 and AZ91-0.5%Ca alloys in as-cast and solution-treated states. AC and ST denote as-cast and solution-treated states, respectively

#### 4. Conclusions

The effects of solution treatment on the microstructure and room temperature mechanical properties were investigated in AZ91 and AZ91-0.5%Ca alloys. In the as-cast state, the Ca addition contributes to the suppression of discontinuous  $\beta$  phase precipitation and the formation of  $Al_2Ca$  phase. After solution treatment, the AZ91 alloy has only a small amount of  $Al_8Mn_5$  particles, while  $\beta$  and  $Al_2Ca$  phases are still present in the Ca-containing alloy. In the as-cast state, the AZ91-0.5%Ca alloy shows better YS and hardness values than does the AZ91 alloy. It is noticeable that the solution treatment results in a marked decrease in YS and hardness in the Ca-free alloy, whereas the decrements in YS and hardness are relatively negligible in the Ca-containing alloy. This result may well be ascribed to the residual compound particles present in the microstructure and solution hardening effect of Ca.

#### Acknowledgement

This study was supported by the Korea Institute of Industrial Technology (KITECH UR-18-0014).

#### REFERENCES

- [1] B.L. Mordike, T. Ebert, *Mater. Sci. Eng. A* **302**, 37 (2001).
- [2] H. Friedrich, S. Schumann, *J. Mater. Proc. Tech.* **117**, 276 (2001).

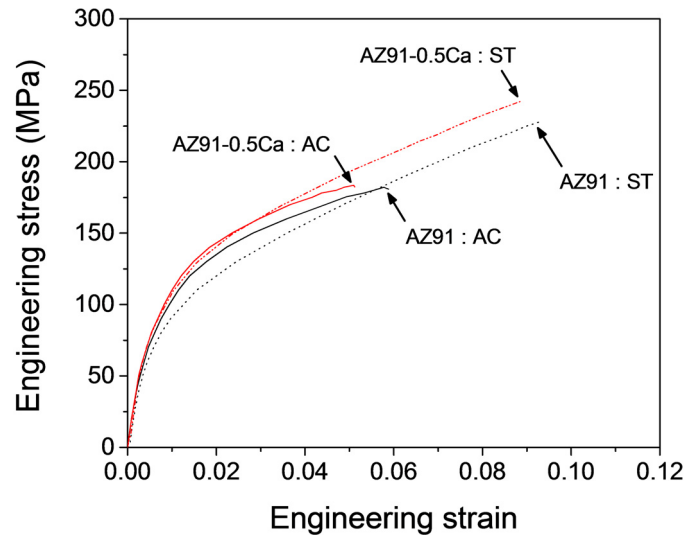


Fig. 5. Engineering stress-strain curves at room temperature of AZ91 and AZ91-0.5%Ca alloys in as-cast and solution-treated states. AC and ST denote as-cast and solution-treated states, respectively

- [3] A. Suzuki, N.D. Saddock, J.W. Jones, T.M. Pollock, *Acta Mater.* **53**, 2823 (2005).
- [4] S. W. Xu, N. Matsumoto, K. Yamamoto, S. Kamado, T. Honda, Y. Kojima, *Mater. Sci. Eng. A* **509**, 105 (2009).
- [5] Y. Terada, N. Ishimatsu, Y. Mori, T. Sato, *Mater. Trans.* **46**, 145 (2005).
- [6] B. Kondori, R. Mahmudi, *Mater. Sci. Eng. A* **527**, 2014 (2010).
- [7] W. Du, Y. Sun, X. Min, F. Xue, M. Zhu, D. Wu, *Mater. Sci. Eng. A* **356**, 1 (2003).
- [8] Y. Nakaura, A. Watanabe, K. Ohori, *Mater. Trans.* **47**, 1031 (2006).
- [9] Q. Wang, W. Chen, X. Zeng, Y. Lu, W. Ding, Y. Zhu, X. Xu, *J. Mater. Sci.* **36**, 3035 (2001).
- [10] Y. Mori, Y. Terada, T. Sato, *Mater. Trans.* **46**, 1749 (2005).
- [11] Y. Terada, N. Ishimatsu, T. Sato, *Mater. Trans.* **48**, 2329 (2007).
- [12] C. H. Caceres, C. J. Davidson, J. R. Griffiths, C. L. Newton, *Mater. Sci. Eng. A* **325**, 344 (2002).
- [13] Y.C. Lee, A.K. Dahle, D.H. StJohn, *Metall. Mater. Trans. A* **31**, 2895 (2000).
- [14] S. Li, B. Tang, D. Zeng, *J. Alloys Compd.* **437**, 317 (2007).
- [15] H. Okamoto, *Desk Handbook Phase Diagrams for Binary Alloys*, ASM International, Ohio (2000). 36.
- [16] H. Okamoto, *Desk Handbook Phase Diagrams for Binary Alloys*, ASM International, Ohio (2000). 27.
- [17] X. Min, Y. Sun, G. Yuan, W. Du, F. Xue: *Chin. J. Nonferr. Met.* **12**, 166 (2002).
- [18] M.A. Gharghoury, G.C. Weatherly, J.D. Embury, J. Root, *Phil. Mag. A* **79**, 1671 (1999).
- [19] M. Song, *Trans. Nonferrous Met. Soc. China* **19**, 1400 (2009).